Supplementary Materials: Alpine Forest Drought Monitoring in South Tyrol: PCA Based Synergy between scPDSI Data and MODIS Derived NDVI and NDII7 Time Series

Katarzyna Ewa Lewińska, Eva Ivits, Mathias Schardt and Marc Zebisch

Table S1. Complete list of meteorological stations used in the study with station number (corresponds with Figure 1), name of the location (in Italian), elevation and length of records used in the survey.

Station Number	Name (Italian)	Elevation (m asl)	Records Since (January)
250	Monte Maria	1310	1967
970	Silandro	698	1988
1120	Diga di Gioveretto	1851	1973
1580	Vernago-Finale	1950	1967
1930	Naturno	541	1973
2090	Plata	1147	1936
2320	Merano-Quarazze	330	1983
2580	Diga di Zoccolo	1144	1979
3260	Vipiteno	948	1935
3360	Diga di Vizze	1365	1973
3450	Ridanna	1350	1969
3910	Bressanone	560	1971
4080	Dobbiaco	1220	1967
4450	S.Maddalena in Casies	1398	1967
4760	Anterselva di Mezzo	1236	1941
5050	Predoi	1449	1980
5980	Brunico	821	1986
6150	La Villa in Badia	1390	1987
6560	Terento	1349	1981
6650	Fundres	1159	1977
7490	Ponte Gardena	490	1984
7560	Fie allo Sciliar	840	1956
8220	Sarentino	966	1977
8320	Bolzano	254	1949
8680	Ora	250	1983
9150	Sesto	1310	1956

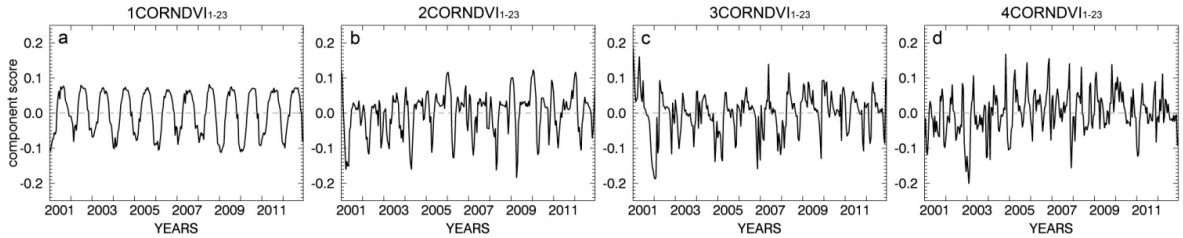

Figure S1. First four PCs resulted from the S-mode correlation-matrix based PCA of the $NDVI_{1–23}$ (full year NDVI) time series, herein: (**a**) $1CORNDVI_{1–23}$; (**b**) $2CORNDVI_{1–23}$; (**c**) $3CORNDVI_{1–23}$ and (**d**) $4CORNDVI_{1–23}$. Temporal patterns explained 63.23%, 3.29%, 2.68% and 1.69% of the total $NDVI_{1–23}$ time series variance respectively.

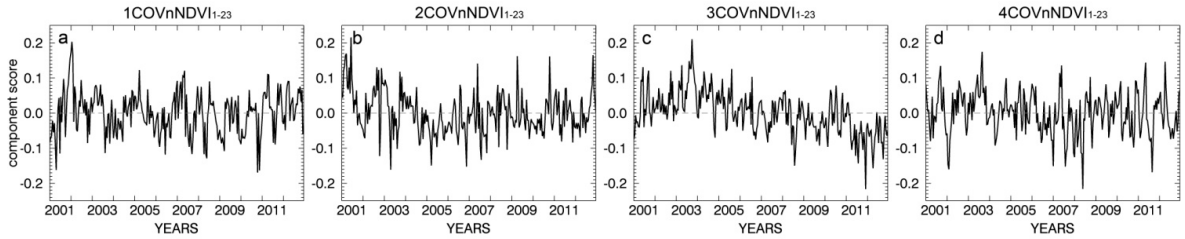

Figure S2. First four PCs resulted from the S-mode covariance-matrix based PCA of the nNDVI$_{1–23}$ (full year z-score normalized NDVI) time series, herein: (**a**) 1COVnNDVI$_{1–23}$; (**b**) 2COVnNDVI$_{1–23}$; (**c**) 3COVnNDVI$_{1–23}$ and (**d**) 4COVnNDVI$_{1–23}$. Temporal patterns explained 18.55%, 5.35%, 2.31% and 1.79% of the total nNDVI$_{1–23}$ time series variance respectively.

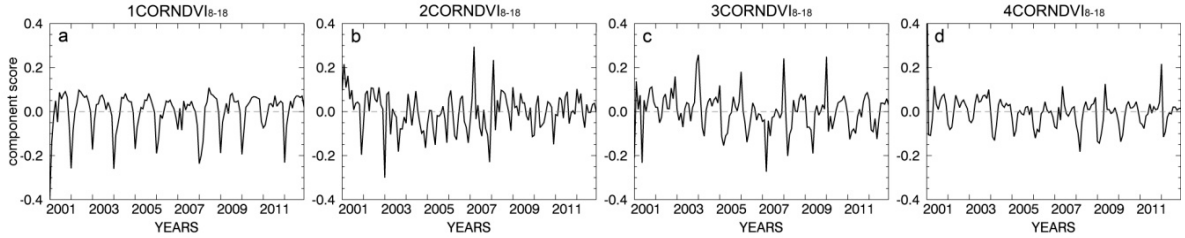

Figure S3. First four PCs resulted from the S-mode correlation-matrix based PCA of the NDVI$_{8–18}$ (vegetation season NDVI) time series, herein: (**a**) 1CORNDVI$_{8–18}$; (**b**) 2CORNDVI$_{8–18}$; (**c**) 3CORNDVI$_{8–18}$ and (**d**) 4CORNDVI$_{8–18}$. Temporal patterns explained 41.94%, 4.77%, 3.04% and 2.68% of the total NDVI$_{8–18}$ time series variance respectively.

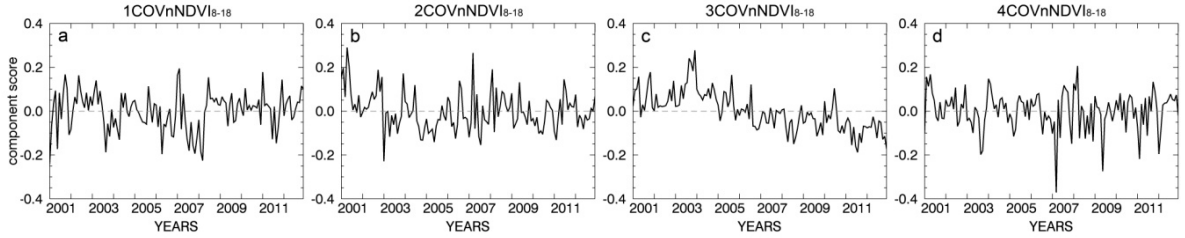

Figure S4. First four PCs resulted from the S-mode covariance-matrix based PCA of the nNDVI$_{8–18}$ (z-score normalized vegetation season NDVI) time series, herein: (**a**) 1COVnNDVI$_{8–18}$; (**b**) 2COVnNDVI$_{8–18}$; (**c**) 3COVnNDVI$_{8–18}$ and (**d**) 4COVnNDVI$_{8–18}$. Temporal patterns explained 15.25%, 5.65%, 3.37% and 2.28% of the total nNDVI$_{8–18}$ time series variance respectively.

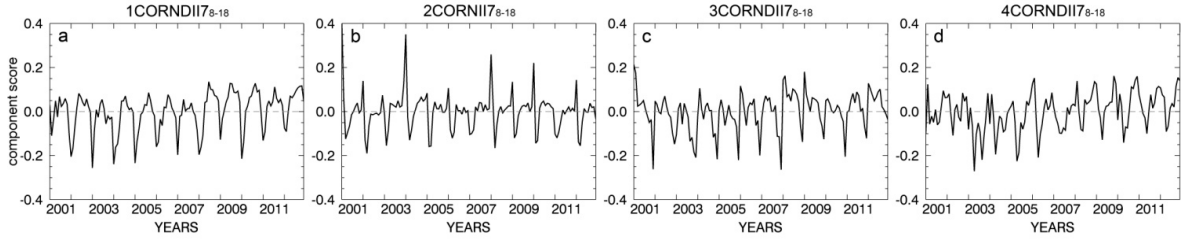

Figure S5. First four PCs resulted from the S-mode correlation-matrix based PCA of the NDII7$_{8–18}$ (vegetation season NDII7) time series, herein: (**a**) 1CORNDII7$_{8–18}$; (**b**) 2CORNDII7$_{8–18}$; (**c**) 3CORNDII7$_{8–18}$ and (**d**) 4CORNDII7$_{8–18}$. Temporal patterns explained 22.55%, 8.66%, 4.40% and 2.68% of the total NDII7$_{8–18}$ time series variance respectively.

Table S2. Correlation between the scPDSI scores and first four PCs obtained through the S-mode (**a**) correlation-matrix based PCA of the $NDVI_{1–23}$ (full year NDVI) time series; (**b**) covariance-matrix based PCA of the $nNDVI_{1–23}$ (full year normalized NDVI) time series; (**c**) correlation-matrix based PCA of the $NDVI_{8–18}$ (vegetation season NDVI) time series; (**d**) covariance-matrix based PCA of the $nNDVI_{8–18}$ (vegetation season normalized NDVI) time series; (**e**) correlation-matrix based PCA of the $NDII7_{8–18}$ (vegetation season NDII7) time series; (**f**) covariance-matrix based PCA of the $nNDII7_{8–18}$ (vegetation season normalized NDII7) time series. Due to inconsistent length of scPDSI, as well as NDVI and NDII7 based datasets all time evolution patterns were converted into yearly average time series.

	(**a**)			
	CORNDVI$_{1–23}$			
	1CORNDVI$_{1–23}$	**2CORNDVI$_{1–23}$**	**3CORNDVI$_{1–23}$**	**4CORNDVI$_{1–23}$**
1scPDSI	0.179	0.215	0.664 *	−0.205
2scPDSI	−0.268	0.476	−0.112	−0.461
3scPDSI	−0.008	0.584 *	−0.460	−0.290
4scPDSI	−0.397	0.215	−0.124	−0.491
	(**b**)			
	COVnNDVI$_{1–23}$			
	1COVnNDVI$_{1–23}$	**2COVnNDVI$_{1–23}$**	**3COVnNDVI$_{1–23}$**	**4COVnNDVI$_{1–23}$**
1scPDSI	0.031	0.712 *	−0.456	−0.070
2scPDSI	−0.263	0.517	0.265	0.181
3scPDSI	0.033	0.195	0.731 *	0.024
4scPDSI	−0.535	−0.278	0.086	0.414
	(**c**)			
	CORNDVI$_{8–18}$			
	1CORNDVI$_{8–18}$	**2CORNDVI$_{8–18}$**	**3CORNDVI$_{8–18}$**	**4CORNDVI$_{8–18}$**
1scPDSI	0.062	0.825 *	0.213	−0.384
2scPDSI	0.082	0.450	0.420	−0.392
3scPDSI	−0.474	0.120	0.457	−0.195
4scPDSI	0.309	0.054	0.364	−0.423
	(**d**)			
	COVnNDVI$_{8–18}$			
	1COVnNDVI$_{8–18}$	**2COVnNDVI$_{8–18}$**	**3COVnNDVI$_{8–18}$**	**4COVnNDVI$_{8–18}$**
1scPDSI	0.573	0.713 *	−0.310	0.374
2scPDSI	0.321	0.608 *	0.360	0.349
3scPDSI	−0.155	0.337	0.632 *	0.160
4scPDSI	0.489	−0.013	0.257	0.261
	(**e**)			
	CORNDII7$_{8–18}$			
	1CORNDII7$_{8–18}$	**2CORNDII7$_{8–18}$**	**3CORNDII7$_{8–18}$**	**4CORNDII7$_{8–18}$**
1scPDSI	0.736 *	0.153	0.660 *	0.702 *
2scPDSI	−0.172	−0.093	−0.193	−0.011
3scPDSI	−0.576 *	0.335	−0.238	−0.386
4scPDSI	0.030	−0.092	−0.050	−0.063
	(**f**)			
	COVnNDII7$_{8–18}$			
	1COVnNDII7$_{8–18}$	**2COVnNDII7$_{8–18}$**	**3COVnNDII7$_{8–18}$**	**4COVnNDII7$_{8–18}$**
1scPDSI	0.717 *	−0.374	0.189	0.608 *
2scPDSI	−0.199	−0.278	−0.260	0.502
3scPDSI	−0.559	0.257	0.131	−0.023
4scPDSI	−0.010	−0.243	−0.288	0.583 *

*—significant at the level $p < 0.05$.

Table S3. Correlation based comparison between first four corresponding PCs derived from Varimax (V) and Promax (P) rotations (ROT) of (**a**) the first five loadings of the COVnNDVI$_{8–18}$ dataset (covariance-matrix based S-mode PCA decomposition of the normalized vegetation season NDVI time series) and (**b**) the first four loadings of the COVnNDII7$_{8–18}$ dataset (covariance-matrix based S-mode PCA decomposition of the normalized vegetation season NDII7 time series).

(**a**)		
PCs	**Correlation**	p
1COVnNDVI$_{8–18}$ROT5V vs. 1COVnNDVI$_{8–18}$ROT5P	0.904	0.000
2COVnNDVI$_{8–18}$ROT5V vs. 2COVnNDVI$_{8–18}$ROT5P	0.890	0.000
3COVnNDVI$_{8–18}$ROT5V vs. 3COVnNDVI$_{8–18}$ROT5P	0.902	0.000
4COVnNDVI$_{8–18}$ROT5V vs. 4COVnNDVI$_{8–18}$ROT5P	0.867	0.000
(**b**)		
PCs	**Correlation**	p
1COVnNDII7$_{8–18}$ROT4V vs. 1COVnNDII7$_{8–18}$ROT4P	0.910	0.000
2COVnNDII7$_{8–18}$ROT4V vs. 2COVnNDII7$_{8–18}$ROT4P	0.897	0.000
3COVnNDII7$_{8–18}$ROT4V vs. 3COVnNDII7$_{8–18}$ROT4P	0.919	0.000
4COVnNDII7$_{8–18}$ROT4V vs. 4COVnNDII7$_{8–18}$ROT4P	0.924	0.000

*—significant at the level $p < 0.05$.

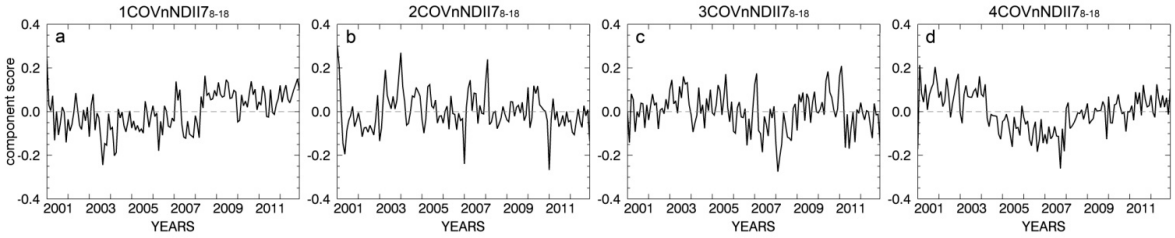

Figure S6. First four PCs resulted from the S-mode covariance-matrix based PCA of the nNDII7$_{8–18}$ (z-score normalized vegetation season NDII7) time series, herein: (**a**) 1COVnNDII7$_{8–18}$; (**b**) 2COVnNDII7$_{8–18}$; (**c**) 3COVnNDII7$_{8–18}$ and (**d**) 4COVnNDII7$_{8–18}$. Temporal patterns explained 11.98%, 3.39%, 2.23% and 1.66% of the total nNDII7$_{8–18}$ time series variance respectively.

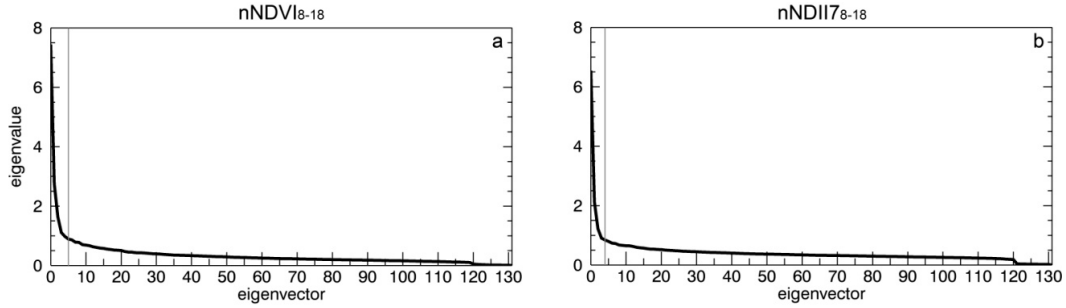

Figure S7. Plots of eigenvalues of (**a**) the covariance-matrix based PCA decomposition of the nNDVI$_{8–18}$ (vegetation season normalized NDVI) time series; and (**b**) covariance-matrix based PCA decomposition of the nNDII7$_{8–18}$ (vegetation season normalized NDII7) time series. Vertical lines represents cutoff value of the Cattell's scree test: 5 and 4 for (**a**) and (**b**) respectively.

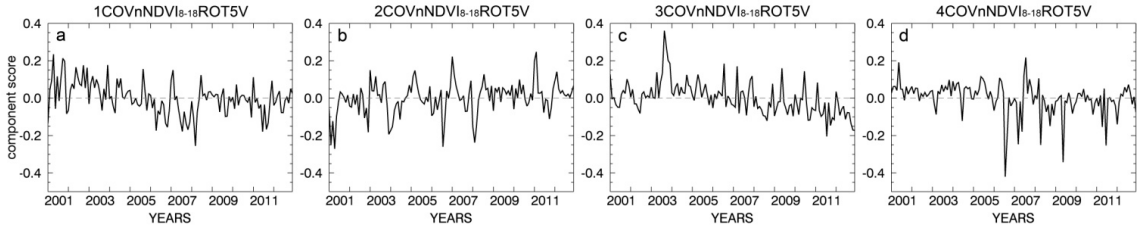

Figure S8. First four PCs (from (**a**) to (**d**) in increasing order) resulted from the Varimax rotation of the first five loadings of the lowest order retained from the COVnNDVI$_{8–18}$ PCA results (covariance-matrix based S-mode PCA of the z-score normalized vegetation-season NDVI time series).

Table S4. Correlation among the scPDSI scores and first four PCs obtained from Varimax (V) and Promax (P) rotations (ROT) of (**a**) the first five loadings of the COVnNDVI$_{8–18}$ dataset (covariance-matrix based S-mode PCA of the normalized vegetation season NDVI time series) and (**b**) the first four loadings of the COVnNDII7$_{8–18}$ dataset (covariance-matrix based S-mode PCA of the normalized vegetation season NDII7 time series. Due to inconsistent length of scPDSI, nNDVI$_{8–18}$ and nNDII7$_{8–18}$ datasets all time evolution patterns were converted into yearly average time series.

(**a**)

	COVnNDVI$_{8–18}$ROT5V				COVnNDVI$_{8–18}$ROT5P			
	1PC	**2PC**	**3PC**	**4PC**	**1PC**	**2PC**	**3PC**	**4PC**
1scPDSI	0.308	−0.203	−0.569	−0.104	0.290	−0.124	−0.590 *	−0.205
2scPDSI	0.638 *	−0.495	0.107	0.353	0.615 *	−0.536	0.186	0.333
3scPDSI	0.476	−0.588 *	0.533	0.380	0.504	−0.576 *	0.607 *	0.324
4scPDSI	0.503	0.057	0.057	0.532	0.433	0.020	0.029	0.612 *

(**b**)

	COVnNDII7$_{8–18}$ROT4V				COVnNDII7$_{8–18}$ROT4P			
	1PC	**2PC**	**3PC**	**4PC**	**1PC**	**2PC**	**3PC**	**4PC**
1scPDSI	0.072	−0.121	−0.548	0.751 *	0.061	−0.254	−0.550	0.772 *
2scPDSI	0.614 *	−0.294	0.143	0.301	0.689 *	−0.427	0.172	0.241
3scPDSI	0.396	0.410	0.200	−0.331	0.365	0.172	0.260	−0.397
4scPDSI	0.527	−0.267	0.090	0.466	0.515	−0.321	0.066	0.400

*—significant at the level $p < 0.05$.

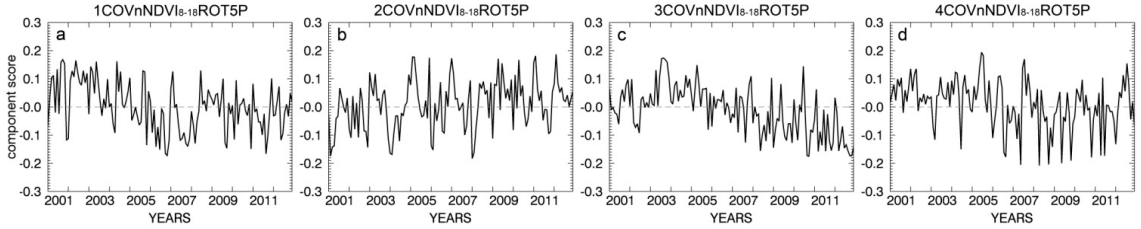

Figure S9. First four PCs (from (**a**) to (**d**) in increasing order) resulted from the Promax rotation of the first five loadings of the lowest order retained from the COVnNDVI$_{8–18}$ PCA results (covariance-matrix based S-mode PCA of the z-score normalized vegetation season NDVI time series).

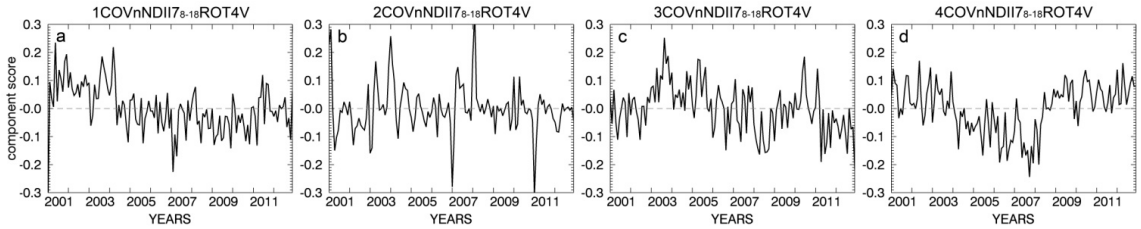

Figure S10. First four PCs (from (**a**) to (**d**) in increasing order) resulted from the Varimax rotation of the first four loadings of the lowest order retained from the COVnNDII7$_{8–18}$ PCA results (covariance-matrix based S-mode PCA of the z-score normalized vegetation season NDII7 time series).

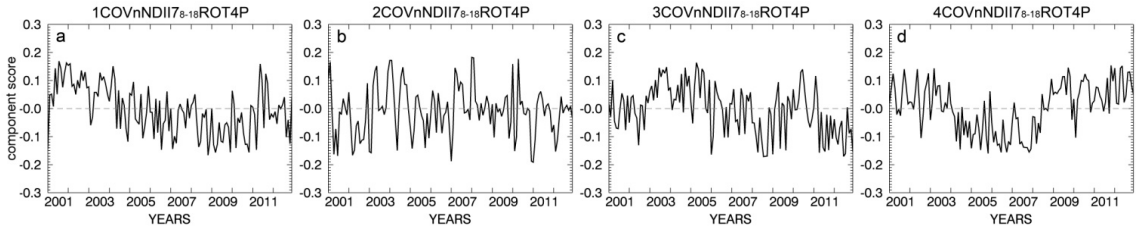

Figure S11. First four PCs (from (**a**) to (**d**) in increasing order) resulted from the Promax rotation of the first four loadings of the lowest order retained from the COVnNDII7$_{8–18}$ PCA results (covariance-matrix based S-mode PCA of the z-score normalized vegetation season NDII7 time series).